Interactive simulation and comparative visualisation of the bone-determined range of motion of the human shoulder

Peter R. Krekel* Charl P. Botha* Edward R. Valstar†
Paul W. de Bruin† P.M. Rozing† Frits H. Post*

Abstract

Pre-operative planning systems aid clinicians by giving insight into patient-specific issues before surgery is performed. The ability to perform a virtual shoulder replacement procedure enables the surgeon to explore the probable and plausible outcomes. Pre-operative planning software assists the surgeon in this complex decision-making process.

In our prototype pre-operative planning system for shoulder replacement, we create patient-specific bone-determined range of motion (ROM) predictions based on collision detection using segmented CT-data. The gleno-humeral ROM is visualised with motion envelopes, that indicate the maximum range of motion of the humerus in every direction. The prosthesis placement parameters can be adjusted interactively in our simulator, during which a novel visualisation technique depicts the differences between the current and previous range of motion.

In this paper we present a fast and efficient method for highly interactive visualisation of collision detection based ROM for the gleno-humeral joint. We are able to show in real-time the consequences of adjustments made to a planned shoulder prosthesis alignment by using geometry clipping-based optimisation, as well as precalculation and interpolation techniques.

1 Introduction

Osteoarthrosis and rheumatoid arthritis, the two most common forms of arthritis, can lead to severe joint damage. The resulting pain and limited joint motion significantly restrict the patient in performing daily activities. In such cases, a joint replacement, i.e. a surgical procedure where parts of the joint are replaced with artificial components, may be indicated. A successful joint replacement leads to pain relief and improved joint mobility.

Replacement operations have a high success rate in the case of the hip or the knee joint. In the case of the shoulder, however, the procedure is often successful with regard to pain relief, but far less successful with regards to post-operative joint mobility or the durability of the implant. The extra complicating factors are the higher complexity of the shoulder

*Data Visualisation Group, Delft University of Technology, The Netherlands, http://visualisation.tudelft.nl/
†Department of Orthopaedics, Leiden University Medical Centre, The Netherlands

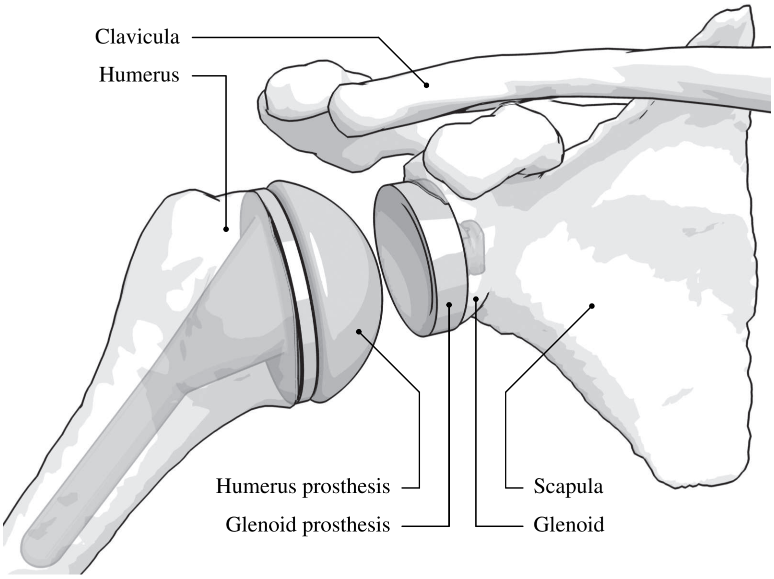

Figure 1: Illustration of a shoulder joint after total shoulder replacement.

joint and the limited field of view during surgery. Our primary motivation for developing a pre-operative planning system is to assist surgeons in performing the difficult shoulder replacement operation, and thereby helping to improve the success rate.

In a total shoulder replacement, the humeral head and the glenoid fossa are replaced with artificial components, as shown in Figure 1. The standard technique for planning a shoulder replacement is template-over-x-ray planning, which involves overlaying several transparent templates of different prostheses on radiographs of the shoulder to determine an appropriate prosthesis. However, the radiographs lack spatial information along the view direction, leading to visual ambiguities that complicate the planning. Our prototype shoulder replacement pre-operative planning system improves on this by allowing the surgeon to simulate the surgery in 3-D. Patient-specific information is extracted from a pre-operative CT scan. During the simulation, the system gives feedback on the surgeon's virtual surgery with regards to the predicted outcome of the operation.

An important aspect of this feedback is the interactive simulation and visualisation of the post-operative bone-determined range of motion of the patient's shoulder. This functionality allows the surgeon to experiment with different prosthesis implantation possibilities and see, in real-time, what the effect of the changes would be on the post-operative bone-determined ROM. The interactive patient-specific ROM simulation and visualisation is the main subject and contribution of this paper.

The remainder of this paper is organized as follows: In section 2 we discuss existing work in the area of pre-operative arthroplasty simulation. Section 3 describes the simulation of bone-determined ROM for the gleno-humeral joint, followed by section 4 where visualisation of ROM envelopes and comparative ROM visualisation is discussed. In section 5 we explain the techniques we apply to enable fast updates of the comparative ROM visualisation, which greatly improves the interactivity of our simulator. We present our results in section 6, followed by our conclusions and discussion of future work in section 7.

2 Related Work

A wide range of pre-operative planning systems exist, for example Hip-Op [LPQ+02], HipNav [SJB+97] and BrainLAB's VectorVision[1]. However, to our knowledge no such specific planning system for the shoulder joint is available at this time. Probable factors here are the complexity and the relatively lower number of replacements of the shoulder joint.

Some research has been done on pre-operative ROM estimation for the hip joint. [JNSDG97] uses analytical modeling of the properties of implants to estimate both the ROM and the chance of dislocation, with bony impingement hardly playing a part. The approach of [RTE+98] resembles our approach more closely, by applying collision detection to the 3D problem of bony impingement. Their system is designed for osteotomy rather than joint replacement and only determines ROM for joint rotation along a single user-defined axis.

The goal of the Comprehensive Human Animation Resource Model (CHARM) project was "modelling a 3D solid human body part with its interior details and having physically based simulation of movements and deformations" [MIR]. The emphasis of this project was on animation, rather than patient-specific ROM prediction. For further reference, see [Mau99].

Lastly, the Delft Shoulder and Elbow Model (DSEM) [vdH94] is a complete musculoskeletal model of the shoulder and elbow joint that mainly focusses on muscle function and the involved forces and energy. However, the DSEM is not patient-specific and therefore not yet usable for pre-operative planning.

3 ROM simulation

In order to calculate the ROM using a segmented CT dataset, we implemented a simplified bio-mechanical model of the gleno-humeral joint. A generally accepted hypothesis is that the gleno-humeral joint can be approximated by a ball-joint [MvdHRR98, vdGVBV02]. We combined this model with collision-detection on surface models of the skeletal structures in the patient's shoulder.

The surface models are extracted from CT data using the segmentation techniques described in chapter 4 of [Bot05]. With this approach, it is possible to extract accurate and topologically correct surfaces describing the skeletal structures of the shoulder from CT data. The techniques are also able to cope with arthritic shoulders where joint space narrowing has occurred or the bone density has been affected. Conventional techniques, such

[1] `http://www.brainlab.com/`

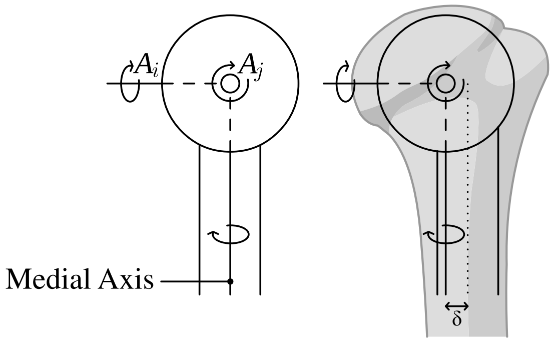

Figure 2: A schematic representation of the humerus and its rotational axes. As can be seen in this image, the additional range of motion as the result of endo/exorotation is related to δ, the distance between the medial axis of the humerus and the vertical axis through the center of rotation.

as double thresholding followed by region growing, do not work in such cases. Shoulder replacement patients often suffer from both these symptoms.

During interactive simulation, we do not take into account rotation around the medial axis of the humerus, i.e. endo/exorotation, thereby reducing the number of degrees of freedom from three to two and greatly speeding up the simulation. This is a reasonable simplification for the following reasons:

- For a healthy joint, the amount of ROM gained as a result of endorotation and exorotation is only discernible in the upper extremes of the gleno-humeral joint. During abductive arm movements, exorotation of the humerus is a common response to be able to reach higher, though most of that particular ROM increase is coming from the scapulo-thoracic joint.
- The maximum achievable ROM increase due to exorotation is relatively small. It is related to the offset of the medial axis of the humerus in relation to the center of rotation, as can be seen in Figure 2.
- Our simulation gives a conservative estimate of the shoulder ROM.

For testing purposes, we have included functionality in our simulator to determine and visualise the extra range of motion gained by a single, adjustable exorotation angle. This enabled us to confirm the above-stated assumptions.

The center of rotation of the gleno-humeral joint is defined by the diameter of the humeral prosthesis, which has a spherical head. Therefore, adjustments made to the prosthesis also affect the center of rotation. For initial placement of the humeral prosthesis, we have implemented a sphere-fitting method. This entails that a sphere is fit over the humeral head to approximate the ideal center of rotation, while continuously giving feedback on how much of the sphere surface is near or touching the humerus surface.

Additionally, our simulator is capable of handling hemi-protheses, which is a prosthesis without a glenoid component, and reversed prostheses, where the spherical component is placed at the glenoid. For the latter, the center of rotation is situated more inward.
For all prostheses, the ROM envelopes are constructed in the following way. The humerus is aligned with an initial orientation, which will be the starting alignment for all iterations. The simulation consists of two nested iterations. During the outer iteration, the humerus is rotated around the axis marked with A_i in figure 2. Note that axis A_j rotates along with A_i. At each rotation, the maximum possible orientation of the humerus around axis A_j is found by making use of a binary search. By repeatedly dividing the search interval in half, our ROM determination executes in $O(\log n)$, where n relates to the effective resolution of the end result of the binary search. Whenever colliding polygons are detected, we reverse the search direction. After an evaluation of available collision detection libraries [Kre05], we selected the Optimized Collision Detection library, or OPCODE [Ter01]. OPCODE is a fast and accurate collision detection library based on memory-optimised bounding-volume hierarchies and most suitable for our particular problem domain. The pseudo-code version of the ROM determination procedure can be seen in Algorithm 1. The algorithm is also explained in Figure 3. For every change in the planning, the complete ROM has to be recalculated.
For hemi-protheses an extra step is required. The humeral head should make contact with the glenoid at all times. Therefore, the humerus has an additional binary search iterator for a translational component as well, rather than just for the rotational extremes. This is not necessary for total shoulder prostheses, as we are targeting conformal prostheses, where the diameters of the glenoid and humerus components are equal. However, using the hemi-prosthesis modelling functionality, our system should be able to simulate non-conformal prostheses as well.

4 Visualisation

Once all directions of our ROM envelope have been probed for their maximum angles, we can begin constructing the ROM visualisation. We draw lines between the center of rotation and an arbitrary point within the end of the shaft of the humerus, and then transform these lines according to their respective maximum angles. The resulting envelope is shown in Figure 4.
For each change made to the virtual prosthesis placement by the surgeon, a new ROM envelope is calculated. This enables the surgeon to visualise directly the complete shoulder range of motion for a particular set of operational parameters. Being able to see the envelope update in real-time as changes are being made, helps the surgeon to investigate the effect of even small changes to the planned operation.
Several parameters that define the placement of the humerus prosthesis can be adjusted during the interaction. First of all, the cutting plane at the humeral head can be translated along its normal, as well as rotated around two axes perpendicular to the normal. Also, the position of the humerus prosthesis relative to the humerus can have a small offset in any direction within the cutting plane. These adjustments are also illustrated in figure 6.

Algorithm 1 The ROM determination algorithm.

```
function DetermineROM(resolution, angle, angle_increment)
i ← 0
while i < 360 do
  t_angle ← angle
  t_angle_increment ← angle_increment
  while (abs(t_angle_increment)> e) do        // e is a threshold for t_angle_increment
    SetOrientation(0,0,0)                     // Set the humerus to an initial orientation
    RotateZ((i/resolution) * 360)
    RotateY(t_angle)
    RotateZ(-(i/resolution) * 360)
    if CDQuery()> 0 then                      // There are colliding polygons
      t_angle_increment ← -abs(t_angle_increment)    // Make the increment negative
    else
      t_angle_increment ← abs(t_angle_increment)     // Make the increment positive
    end if
    t_angle_increment ← t_angle_increment ×0.5       // Cut increment in half
    t_angle ← t_angle+t_angle_increment    // Add the increment to the previous angle
  end while
  AddToArray(t_angle)
  i ← i + 360/resolution                      // Proceed to the next direction
end while
```

The ROM determination algorithm. The auxiliary function *CDQuery* returns the number of colliding polygons. The parameters $resolution$, $angle$ and $angle\_increment$ are adjustable and define the number of envelope lines, the initial angle we use for our simulation and the increment we add to the previous angle at each iteration, respectively. Also, the search range depends on these three parameters.

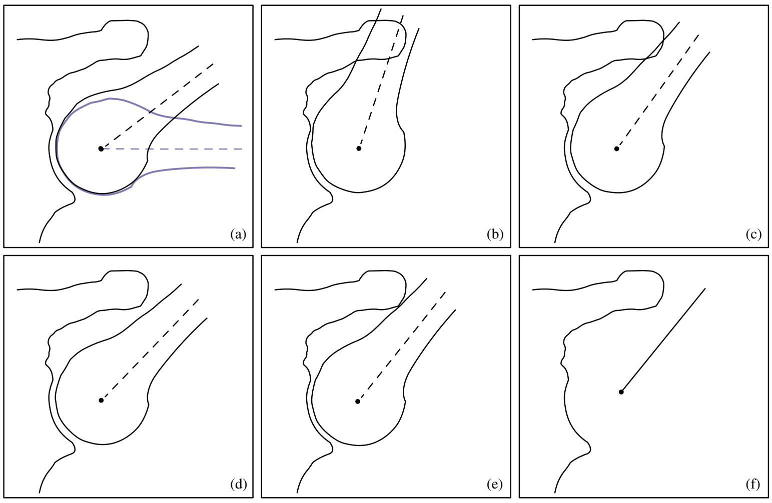

Figure 3: Binary search algorithm for one line of the ROM envelope. The blue humerus (a) represents the initial orientation. At each iteration, the increment is added to the previous angle (a, d, e) and halved. If colliding polygons are detected, the increment is preceded by a negation (b, c). If the increment is smaller than a certain threshold, the line is added to the envelope (f).

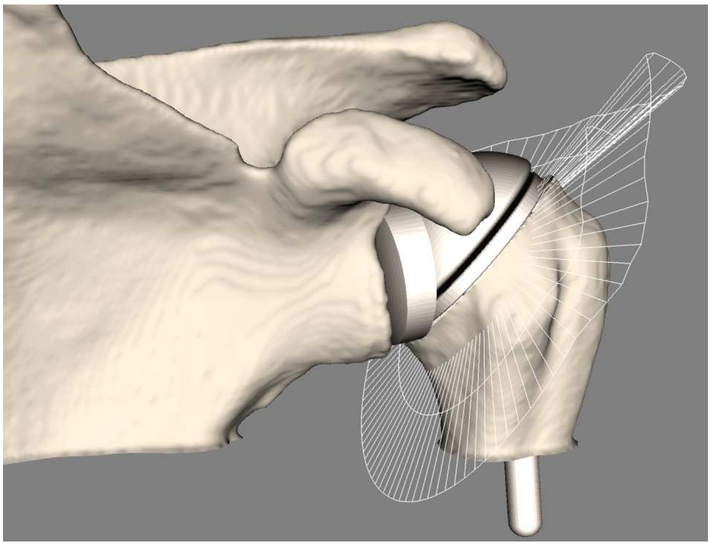

Figure 4: The visualisation of ROM by means of envelopes.

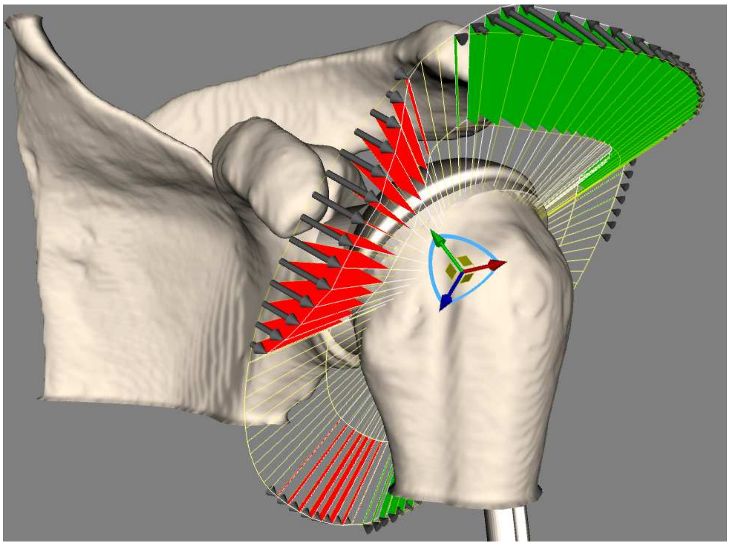

Figure 5: Comparative visualisation of two ROM envelopes. The first envelope is a previously determined ROM which was set as a reference envelope by the user. The second envelope is continuously updated for every adjustment applied to the prosthesis placement parameters.

Placement of the glenoid prosthesis is performed according to a method described in section 3.1 of [Bot05]. It is quite strictly constrained by the quality and the geometry of the scapula. Therefore, we focused on the alignment of the humeral prosthesis.

In order to facilitate this important investigation of the increase or decrease in range of motion that results from a particular change in the planning, we have implemented comparative visualisation functionality whereby the difference between two ROM envelopes can be explicitly visualised. The comparative visualisation is also updated in real-time as the surgeon interacts with the planning.

For two consecutive envelopes we depict improvements and deteriorations by connecting the lines with colored polygons. A red polygon denotes that the most recent envelope has a more limited ROM in that particular direction than the reference envelope, while a green polygon states the opposite. Additionally, the end points of the lines are connected with arrows, pointing towards the most recent envelope. The resulting visualisation is shown in Figure 5. The reference envelope can be set to the current or any previously determined ROM envelope at all times.

5 Optimisation

To support the interactive usage of our system, we focussed on decreasing the time required to display consecutive ROM envelopes during prosthesis placement adjustments. We have

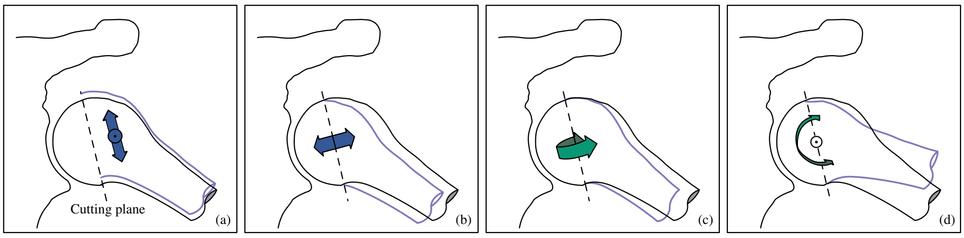

Figure 6: These are the possible placement adjustments, that are also systematically modified during precalculation. In (a) we see the humerus, which can be translated along the cutting plane. In (b) it is translated along the normal of the cutting plane. In (c) and (d) we see the two axes used for orientation changes. Note that all adjustments are applied to the humerus only, thereby changing its position relative to the prosthesis.

implemented two kinds of optimisations. Only one optimisation should be picked, depending on the intentions of the user. The first optimisation is based on precalculation and aims at a thorough exploration of the ROM for a single prosthesis. The second optimisation is based on geometry clipping and more suitable for comparison of the ROM of different prosthesis types. When no time is available for precalculation, this optimisation should be selected.

We describe both these optimisation methods in the following two subsections. In section 6, we show the results of performance and accuracy measurements on our simulator with and without optimisation.

5.1 Precalculation and interpolation

To ensure a satisfactory frame-rate, we optimised the simulation through precalculation and interpolation techniques. During the initialization phase, a variable number of ROM envelopes are precalculated. Depending on the resolution and ranges, this number can vary from 400 to as much as 2000. For a single orientation of the humerus prosthesis, we start by precalculating envelopes for translational adjustments along the cutting plane (see Figure 6a). This is then repeated for translational adjustments along the normal of the cutting plane (Figure 6b). Finally, the previous two steps are repeated for variations of the prosthesis orientation (Figure 6c and d).

Now that we have completed the precalculation step we can interpolate the ROM predictions at a high frame-rate, with only little accuracy loss. When the CPU is idle, the accurate ROM envelope can be calculated and replace the interpolated envelope with a smooth transition.

The drawback of this approach is that the precalculations only hold for a single type and size of a prosthesis. When the surgeon wants to compare the ROM of various prostheses for a particular dataset, precalculation will have to be done for each of those prostheses.

5.2 Collision Clipping

For the concept of collision clipping, we differentiate between placement adjustments that require geometry adaptation (GA) and those that do not. Geometry adaptation is necessary for prosthesis placement adjustments that redefine the cutting plane, relative to the humerus (see Figure 6b, c & d).

A problem with geometry adaptation is that the bounding boxes hierarchy, which is used by the collision detection library, becomes outdated and needs to be rebuilt. This can take up to 3 seconds for high-density models, slowing down the simulation unacceptably.

Instead of performing collision detection queries on the clipped model of the humerus, we use the unclipped model. Thus, our collision detection queries may return collisions of polygons that would normally have been clipped. By adding an additional query to the algorithm, we can find out on which side of the cutting plane the colliding polygons are located. If they are on the same side of the cutting plane as the prosthesis, the collisions are ignored. Otherwise, the algorithm can terminate, since we only need one admissible collision to identify an unacceptable humerus alignment.

Another slow down is caused by the clipping of the humerus model itself. Because we have now separated the graphical representation from the collision detection algorithm, the humerus model does not necessarily have to be clipped, other than for graphical representation purposes. Therefore, we use a much faster graphics hardware geometry cutting plane instead of an accurate clipping algorithm.

6 Results

So far, the prototype system we developed has been tested on two in-vivo shoulder CT datasets of patients requiring total shoulder replacements, with more tests being planned. However, due to the consistent results generated by the specialised segmentation techniques, we do not expect much deviation from these results for other datasets.

An orthopaedic surgeon used our simulator and these datasets for prosthesis placement analysis and stated that the presented ROM estimations correlated with anticipated behaviour. We received positive feedback on the interactively updated comparative visualisations, which was experienced as both fast and intuitive.

The accuracy of the interpolation is dependent on the variable density of precalculated ROM envelopes. For this specific benchmark, we calculated the deviation between various different ROM envelopes that were calculated with and without optimisation. In total, the deviation was measured for 5000 ROM angles. The median deviation was $0°$, the interquartile range (IQR) was $0.15°$ ($0° - 0.15°$) and the maximum absolute deviation was $2.67°$. This deviation is small enough to be justified by the significant interactive speed-increase gained through the optimisation.

We benchmarked the precalculation process as well as the interactive performance of our simulator on a Pentium 4 running at 2.66 GHz with 512 MB of RAM. The humerus model consisted of 50.000 polygons, while the scapula consisted of 155.000 polygons. Precalculation of 1782 complete ROM envelopes took 22 minutes. This has to be performed once per patient shoulder and can be integrated with the CT acquisition workflow.

	With rendering		Without rendering	
	no GA	GA	no GA	GA
no-opt	1.79	0.27	1.93	0.30
coll-clip	2.38 (× 1.33)	2.22 (× 8.22)	2.70 (× 1.40)	2.69 (× 8.97)
interp	19.23 (× 10.74)	10.81 (× 40.04)	388.7 (× 201.4)	374.4 (× 1248)

Table 1: Speed of simulation and rendering in updates per second. *no-opt*, *coll-clip* and *interp* are short for "no optimisation", "collision clipping" and "interpolation" respectively. *Collision clipping* refers to the measure documented in section 5.2. *Interpolation* refers to the measure documented in section 5.1. *GA* refers to "geometric adaptation" (see section 5.2). All performance figures are specified as updates per second, figures in parentheses refer to speedups relative to "no optimisation" performance.

Performance figures for the interactive ROM simulation are listed in Table 1. As can be seen, the speed increase due to collision clipping varies from a factor of 1.33 to 8.22 for normal usage of the simulator. The speed increase due to interpolation varies from a factor of 10.74 to 40.04. If we discard the graphical representation, the speed increase by interpolation gets as high as a factor of 1248. From these results we draw the following conclusions:

First, when no optimisation takes place, adjustments that require the geometry to be modified have a much lower update rate than other adjustments. This originates in the problem of geometry adaptation (described in section 5.2) and results in an update rate of 0.27 updates/s.

Second, the frame-rates of the aforementioned adjustments are substantially higher when we apply the collision clipping optimisation. This optimisation enables interactive usage of our simulator without any form of precalculation. Consequently, we can use this technique to explore and compare the ROM estimations for multiple types and sizes of prostheses.

Third, the speed increase for interpolated ROM envelopes without graphical feedback is extremely large. This can be ascribed to the interpolation process, which is far less computationally expensive than the accurate determination of a single ROM envelope. For unoptimised ROM calculations and collision clipping, hardly anything of the routine is changed when graphical feedback is disabled, explaining the poor speed increase for these categories.

We conclude from these results that both optimisations are very effective. Compared to interpolated ROM estimations, the frame-rate for real-time exploration with collision clipping is on the low side. Perhaps additional speed increase is possible if we use heavily decimated models or limit the search range to areas where problems are likely to occur. Nevertheless, the fact that collision clipping does not require precalculation steps, makes it a good alternative for precalculated ROM predictions.

7 Conclusions and Future Work

In this paper we presented a practical technique for the calculation and visualisation of shoulder range of motion envelopes. We designed an extensive precalculation and interpolation scheme that enables the exploration of a shoulder replacement planning in real-time. For every change made by the surgeon during the pre-operative planning, the resulting range of motion can be interactively visualised. We also employ the graphics hardware clipping plane to achieve interactivity at a lower frame-rate, without the requirement of precalculation.

Because comparing different ROM envelopes is crucial for the evaluation of different pre-operative choices, we implemented a comparative visualisation for ROM envelopes. The comparative visualisation can also be updated interactively and explicitly shows differences in mobility that result from the surgeon's actions during the pre-operative planning.

We performed measurements to show that the difference between interpolated and calculated ROM envelopes is relatively small. Speed measurements showed that the simulator is highly interactive when we apply precalculation and interpolation techniques.

The system we describe in this paper concerns bone-determined ROM, which provides feedback on the risk of impingement. We plan to extend this with information on the presence of muscle tissue, ligaments and cartilage. Alternatively, a model of these aspects could be used, such as the DSEM, described in section 2. While the model would greatly complement our impingement-based ROM system, it is not yet patient-specific [vdHVP+92]. Still, integration of the DSEM is under consideration for future work.

Our simulator is an important component of a pre-operative arthroplasty planning system for the shoulder joint [Bot05]. However, the presented techniques are generic and applicable to other joints as well, such as the hip and knee joint. With regard to the simulator, we will continue to add new functionality and refine existing features to better fit clinical practice, for example expansion of the prostheses database and improvement of user interface elements.

Finally, we plan to perform a validation study on cadaver shoulders, where motion limitation should correspond to the ROM estimations of our simulator.

References

[Bot05] Charl P. Botha. *Techniques and Software Architectures for Medical Visualisation and Image Processing.* PhD thesis, Delft University of Technology, 2005. `http://cpbotha.net/Publications/PhDThesis`.

[JNSDG97] B. Jaramaz, C. Nikou, D. Simon, and A.M. Di Gioia. Range of motion after total hip arthroplasty: Experimental verification of the analytical simulator. Technical Report CMU-RI-TR-97-09, Robotics Institute, Carnegie Mellon University, Pittsburgh, PA, February 1997.

[Kre05] Peter R. Krekel. Collision detection for the pre-operative planning of shoulder arthroplasty. Technical report, Delft University of Technology, 2005.

[LPQ+02] R. Lattanzi, M. Petrone, P. Quadrani, C. Zannoni, and M. Viceconti. Applications of 3d medical imaging in orthopaedic surgery: Introducing the hip-op system. *Proc. First International Symposium on 3D Data Processing Visualization and Transmission*, pages 808–811, June 2002.

[Mau99] Walter Maurel. *3D Modeling of the Human Upper Limb including the Biomechanics of Joints, Muscles and Soft Tissues*. PhD thesis, Ecole Polytechnique Federale de Lausanne, 1999. `http://ligwww.epfl.ch/~maurel/Thesis98.html`.

[MIR] MIRALab. Charm project website. `http://www.miralab.unige.ch/3research/research_project.cfm?projectid=CHARM`.

[MvdHRR98] C.G.M. Meskers, F.C.T. van der Helm, L.A. Rozendaal, and P.M. Rozing. *In vivo* estimation of the glenohumeral joint rotation center from scapular bony landmarks by linear regression. *Journal of Biomechanics*, 31:93–96, 1998.

[RTE+98] J.A. Richolt, M. Teschner, P. Everett, B. Girod, M.B. Millis, and R. Kikinis. Planning and evaluation of reorienting osteotomies of the proximal femur in cases of scfe using virtual three-dimensional models. In *MICCAI '98: Proceedings of the First International Conference on Medical Image Computing and Computer-Assisted Intervention*, pages 1–8, London, UK, 1998. Springer-Verlag.

[SJB+97] D.A. Simon, B. Jaramaz, M. Blackwell, F. Morgan, A.M. DiGioia, E. Kischell, B. Colgan, and T. Kanade. Development and validation of a navigational guidance system for acetabular implant placement. *Proc. of the First Joint CVRMed / MRCAS Conference*, pages 583–592, 1997.

[Ter01] Pierre Terdiman. Memory-optimized bounding-volume hierarchies. 2001. `http://www.codercorner.com/Opcode.htm`.

[vdGVBV02] Marjolein van der Glas, Frans M. Vos, Charl P. Botha, and Albert M. Vossepoel. Determination of Position and Radius of Ball Joints. In Milan Sonka, editor, *Proceedings of the SPIE International Symposium on Medical Imaging*, volume 4684 - Image Processing, 2002.

[vdH94] Frans C.T. van der Helm. A finite element musculo-skeletal model of the shoulder mechanism. *Journal of Biomechanics*, 27(5):551–569, 1994.

[vdHVP+92] F.C.T. van der Helm, H.E. Veeger, G.M. Pronk, L.H. van der Woude, and R.H. Rozendal. Geometry parameters for musculoskeletal modelling of the shoulder mechanism. *Journal of Biomechanics*, 25(2):129–144, February 1992.